# Low-capacity utilization of process plants : a cost-robust approach to tackle man-made domino effects

**Reference:**
Khakzad Nima, Reniers Genserik.- Low -capacity utilization of process plants : a cost-robust approach to tackle man-made domino effects
Reliability engineering and system safety - ISSN 0951-8320 - 191(2019), p. 1-9
Full text (Publisher's DOI): https://doi.org/10.1016/J.RESS.2018.03.030

# Low-capacity utilization of chemical plants: A cost-roust approach to tackle man-made domino effects

Nima Khakzad*, Genserik Reniers

Safety and Security Science Group, Delft University of Technology, The Netherlands.

Corresponding author:

n.khakzadrostami@tudelft.nl

Phone: +31 15 27 84709

Address: Jaffalaan 5, Delft 2628 BX, The Netherlands

## Abstract

Chemical and process plants can be potential targets to terrorist attacks with the aim of triggering domino effects. Compared to accidental domino effects where the possibility of having multiple primary events is very remote, man-made domino effects are likelier to be initiated from multiple units within the plant in order to increase their likelihood and thus causing maximum damage. In this regard, identification of critical units that under attack may lead to likelier and severer domino effects is crucial to assess the vulnerability of chemical plants and subsequently to increase their robustness to such attacks. In the present work, we have developed a methodology based on graph theory for cost-robust design of chemical plants to lower the possibility of intentional domino effects. We have validated the methodology using a Dynamic Bayesian network approach just to find out a complete agreement between the results of the two techniques. The developed graph theoretic methodology is demonstrated to be effective particularly in the case of existing chemical plants where possibility of macro-layout modifications is limited.

**Key words**: Domino effect; Chemical plants; Intentional attack; Graph theory; Dynamic Bayesian network; Robustness.

# Introduction

Chemical and process plants have frequently been the targets of intentional attacks including terrorist attacks, sabotage, vandalism, and insider malicious acts [1]. Intentional attacks, especially those launched by terrorists, are usually aimed at causing maximum damage in terms of, among others, loss of lives and assets. As such, it seems reasonable to expect an "intelligent attacker" to aim for triggering domino effects in chemical facilities. In the chemical and process industries, the term "domino effect" is referred to a chain of fires and/or explosions triggered by a primary fire or explosion at a process vessel [2]. The escalation of primary fire(s) or explosion(s) (primary events) to secondary fires or explosions (secondary events) occurs by means of heat radiation, fire impingement, fire engulfment, blast wave, or projectile fragments, which are known as escalation vectors. Although rare, domino effects have contributed to a number of catastrophic accidents such as explosions at a liquefied petroleum gas facility in Mexico in 1984 [3], fires and explosions at an oil storage terminal in the UK in 2005 [4], and tank farm explosions and fires in Puerto Rico in 2009 [5].

In the case of intentional attacks with improvised explosive devices (IEDs) such as pipe bombs and car bombs, the blast wave of detonation can severely damage process vessels and result in major release of flammable chemicals, which in contact with the heat of detonation, are very likely to ignite, leading to domino effects. Compared to accidental domino effects where the possibility of having multiple primary events is very remote, in intentional domino effects, it is likelier that multiple vessels are simultaneously attacked in order to increase (from the attacker's viewpoint) the possibility and severity of potential domino effects. The recent attack to a French chemical plant in July 2015 [6] is an example of such multi-target attacks in which two chemical storage tanks, nearly 500 m away from each other, were attacked with IEDs leading to tank fires[1].

Due to their catastrophic consequences, many researches have been devoted to modeling and risk assessment of domino effects in chemical and process facilities [7-14]. A multitude of previous work has been devoted to accidental domino effects whereas a few works has been dedicated to intentional or man-made domino effects [15-17]. Comparing intentional and accidental domino effects, aside from the higher likelihood of multiple primary events in the former, the likelihood of targeting the most critical vessels in the former is much higher than the latter. This is because, if the attacker is considered a rational decision maker [18], he plans to maximize the expected utility of his attack [19] via attacking the vessels with the highest possibility of triggering domino effects and thus inflicting maximum damage to the plant. Khakzad and Reniers [20] demonstrated that modeling potential domino effects in a chemical plant as a directed graph, graph centrality scores (graph metrics) such as closeness and betweenness can be used to identify process vessels with the largest contribution to domino effects.

In the present study, we aim to investigate the applicability of graph metrics and Bayesian network to vulnerability assessment and reduction of chemical plants in face of intentional domino effects. The developed methodologies is shown to be effective particularly in modification of existing chemical plants where macro-layout changes cannot easily be implemented. In Section 2, the fundamentals of graph theory, Bayesian network, and multi-criteria decision making are briefly recapitulated. In Section 3, a demonstrative example is used to develop the methodology based on graph theory, followed by its validation using dynamic Bayesian network. Application of the methodology to a case study and the results are in Section 4. The conclusions are drawn in Section 5.

[1] Remainings of some IEDs were also found near a third storage tank though it did not cause any damage.

## Background

### 2.1. Graph theory

Domino effects in a chemical plant can be modeled as a directed graph $G = \{V, E\}$ where the process vessels are considered as the vertices of the graph, $V = \{v_1, v_2, \dots, v_n\}$, and the escalation vectors among the vessels as the edges of the graph, $E = \{e_{12}, e_{13}, \dots, e_{ij}\}$ [20]. For instance, if vessels $v_1$ is on fire, the heat radiation $v_2$ receives from $v_1$ is indicated as $e_{12}$. In a weighted graph, a set of numerical values can be assigned to either the vertices or the edges of the graph. A weighted graph can be presented as $G = \{V, W_v, E, W_e\}$ in which $W_v$ and $W_e$ are weight vectors allocated to the vertices and the edges, respectively.

In a directed graph, a path from $v_i$ to $v_j$ is a sequence of edges starting from the former to the latter when each intermediate vertex can be traversed only once. Similarly, the geodesic distance between the vertices, denoted by $d_{ij} = d(v_i, v_j)$, is the length of the shortest path from $v_i$ to $v_j$.

Based on the concept of geodesic distance, a number of graph metrics can be used to describe the characteristics of either the nodes of a graph or the graph itself [21]. Among such metrics, closeness centrality scores are very popular. The out-closeness of $v_i$, $C_{out}(v_i)$, can be defined as the number of steps needed to reach every other node of the graph from $v_i$; the in-closeness $C_{in}(v_i)$, on the other hand, is the number of steps needed to reach $v_i$ from every other node of the graph:

$$C_{out}(v_i) = \frac{1}{\sum_j d_{ij}} \tag{1}$$

$$C_{in}(v_i) = \frac{1}{\sum_j d_{ji}} \tag{2}$$

Based on the centrality scores of a graph's nodes given in Equations (1) and (2), the closeness scores, whether out-closeness or in-closeness, of the graph can be measured.

### 2.2. Bayesian network

Bayesian network (BN) is a graphical tool for reasoning under uncertainty [22,23]. In a BN, joint probability distribution of a set of random variables is represented in terms of conditional probabilities. In a BN (Figure 1(a)), random variables are represented by nodes (in the form of ellipse) while the direct dependencies among the nodes are represented by directed arcs. Satisfying the Markov condition – which states that a node (e.g., $X_4$) is independent of its non-descendants (i.e.,

$X_1$ and $X_3$) given its parents (i.e., $X_2$) – a BN factorizes the joint probability distribution of its nodes as the product of the conditional probability distributions of the variables given their parents:

$$P(X_1, X_2, \dots, X_n) = \prod_{i=1}^{n} P(X_i|Pa(X_i)) \tag{3}$$

where $Pa(X_i)$ is the parent set of the variable $X_i$. Considering the BN in Figure 1(a), $P(X_1, X_2, X_3, X_4) = P(X_1)\, P(X_2|X_1)\, P(X_3|X_1,X_2)\, P(X_4|X_2)$.


(a) (b)

**Figure 1**. (a) Bayesian network. (b) Influence diagram.

A BN can be extended to an influence diagram (Figure 1(b)) using two additional types of nodes, decision node D and utility node U [23] in order for decision making. Decision and utility nodes are conventionally displayed as rectangles and diamonds, respectively. A decision node incorporates a number of decision policies. A decision node should be assigned as the parent of nodes the probability distributions of which depend on decision policies (e.g., the arc from the decision node D to $X_2$). Likewise, the decision node should be the child of nodes the states of which have to be known to the decision maker before making decision (e.g., the dashed arc from $X_1$ to the decision node D). The utility node U incorporates utility values (positive or negative) to represent the preferences of the decision maker as to the outcomes of each decision policy.

Considering three decision policies for node $D = \{d_1, d_2, d_3\}$ and a binary node $X_3 = \{x_3^+, x_3^-\}$ in Figure 1(b), node $U$ should include six utility values, one for each pair of decision policies and the states of $X_3$. As such, the expected utility of each decision policy can be calculated; for example, the expected utility of the 2nd decision policy $d_2$ can be calculated as:

$$EU(d_2) = \sum_{X_3} P(X_3|d_2)\, U(d_2, X_3) = P(x_3^+|d_2)\, U(d_2, x_3^+) + P(x_3^-|d_2)\, U(d_2, x_3^-) \tag{4}$$

Assuming a rational decision maker [18], the decision policy with the maximum expected utility can be selected as the optimal decision, $d^*$ [23]:

$$d^* = \underset{d_i}{arg\,max}\, EU(d_i) \quad \text{for } i = 1,2,3 \tag{5}$$

A dynamic Bayesian network (DBN) is a replication of ordinary BN over time, that, compared to its predecessor, facilitates explicit modeling of temporal changes of random variables (Figure 2). Dividing the timeline into a number of time intervals, DBN allows a node at the i$^{th}$ time slice to be conditionally dependent not only on its parents at the same time slice but also on its parents and itself at previous time slices:

$$P(X_1, X_2, \ldots, X_n) = \prod_{i=1}^{n} P(X_i^{t+\Delta t} | X_i^t, \pi(X_i^t), \pi(X_i^{t+\Delta t})) \tag{6}$$

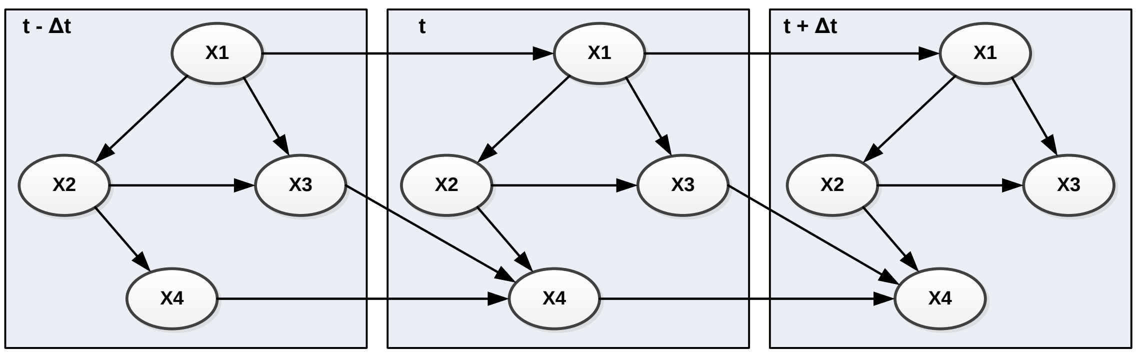


**Figure 2**. Schematics of a dynamic Bayesian network in three sequential time intervals.

According to the DBN in Figure 2, the conditional probability of $X_4$, for example, at the time slice $t + \Delta t$ is $P(X_4^{t+\Delta t} | X_2^{t+\Delta t}, X_3^t, X_4^t)$.

## 2.3. Pareto optimization

In real-life decision making problems, decision criteria that influence the decision making process are usually in conflict. Multi-criteria decision analysis (MCDA) techniques have been developed with the aim of helping decision makers deal with such complex situations. Due to conflicting nature of decision criteria, it is usually unlikely to make a decision which satisfies all the decision criteria. In MCDA, a Pareto-optimal solution is a decision alternative for which there is no other alternatives where the value of a criterion can be improved without worsening or maintaining the value of other criteria. A set of Pareto-optimal solutions refers to a number of such decision alternatives which are normally prioritized based on the preferences of a decision maker.

The method of “reference point” is one of the techniques in bi-criteria decision analysis, which intuitively represents the preferences of a decision maker based on aspiration and reservation vectors [24]. An aspiration vector is composed of the best values of the criteria whereas a reservation vector contains the worst values of the criteria. The aspiration and reservation vectors identify “Utopia” and “Nadir” points, respectively. Optionally, a decision maker can define his preferred solution between aspiration and reservation levels, and based on the distances of Pareto-optimal solutions from Utopia and Nadir points. Figure 3 schematizes a reference point decision making technique, comprising a set of Pareto-optimal solutions, i.e., points A–F, and Utopia and Nadir points. Accordingly, the solution which is the closest/farthest (e.g., using Euclidean distance) to/from the Utopia/Nadir point can be determined as the best solution:

$$\rho_i = \sqrt[2]{(x_i - x_U)^2 + (y_i - y_U)^2} \tag{7}$$

where $\rho_i$ is Euclidean distance of the i$^{th}$ Pareto-optimal point from Utopia point; $x_i$ and $x_U$ are the values of the criterion X of the i$^{th}$ point and Utopia point, respectively; $y_i$ and $y_U$ are the values of the criterion Y of the i$^{th}$ point and Utopia point, respectively. It should be noted that the application of reference point technique implies the equal importance of the decision criteria to the decision maker.

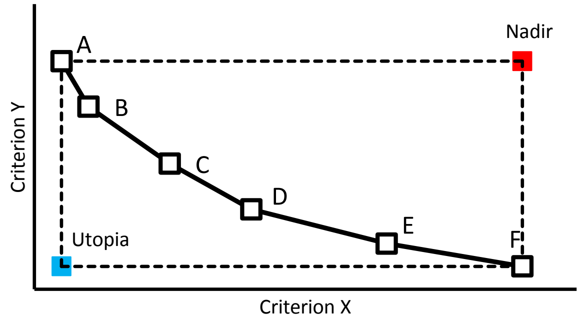


**Figure 3**. Reference-point decision analysis.

# Methodology

## 3.1. Demonstrative example

For the sake of clarity, we use a demonstrative example to help develop the methodology. Figure 4(a) displays a chemical plant consisting of six gasoline storage tanks with a diameter of D= 30.5 m, height of H= 9.1 m, and capacity of V= 8073 $m^3$. Considering tank fires as the likeliest scenario anticipated from an attack with IEDs [6], the amounts of heat radiation Tank Tj receives from Tank Ti are calculated using ALOHA software [25] as reported in Table 1, assuming a wind speed of 2 m/s from NW, 25% relative humidity, and air temperature of 18 C. Since all the vessels are atmospheric, the heat radiation threshold cable of causing damage and thus triggering a domino effect is considered as 15 kW/$m^2$ [11]. As such, heat radiation intensity values less than this threshold are not presented in Table 1.

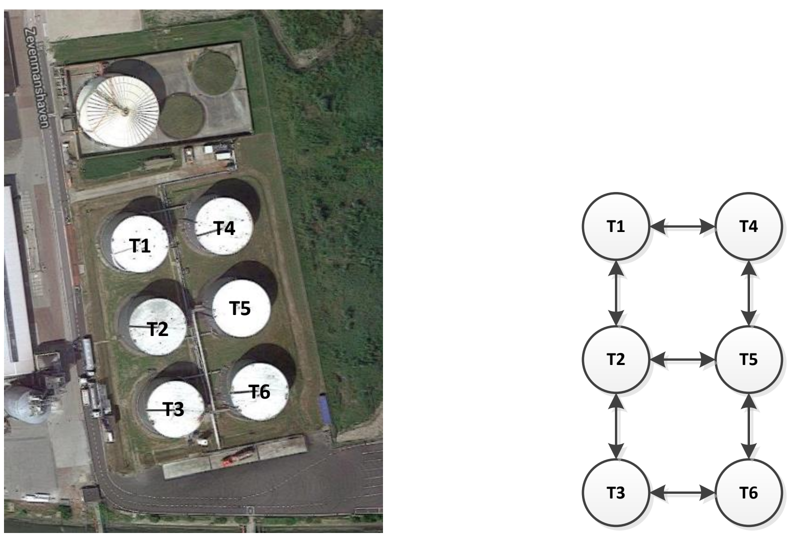


(a) (b)

**Figure 4**. (a) A chemical plant consisting of six gasoline storage tanks. (b) The possible domino effects at the chemical plant as a directed graph.

**Table 1**. Heat radiation intensity (kW/m$^2$) Tj receives from a tank fire at Ti. Values less than 15 kW/m$^2$ are not presented.

| Tj↓ Ti→ | T1 | T2 | T3 | T4 | T5 | T6 |
|---|---|---|---|---|---|---|
| T1 | – | 38 | – | 22 | – | – |
| T2 | 38 | – | 38 | – | 22 | – |
| T3 | – | 38 | – | – | – | 22 |
| T4 | 22 | – | – | – | 38 | – |
| T5 | – | 22 | – | 38 | – | 38 |
| T6 | – | – | 22 | – | 38 | – |

## 3.2. Vulnerability assessment

### 3.2.1. Application of graph metrics

Modeling possible domino effects in a chemical facility as a directed graph (Figure 4(b)), Khakzad and Reniers [20] showed that process vessels with higher out-closeness centrality scores can lead to relatively severer domino effects if ignited or exploded as primary vessels. Following their work in the present study, we aim to investigate if intentional attack to a limited number of process vessels with the highest out-closeness would result in the severest domino effect than attack to any similar number of other process vessels.

To this end, the directed graph in Figure 4(b), which has been drawn based on mutual interactions between the storage tanks in Table 1, is modeled in igraph package [26]. The storage tanks' out-closeness scores are presented in Table 2, indicating T2 and T5 as the tanks with the highest out-closeness. As such, a single attack to T2 or T5 should trigger a severer domino effect than a single attack to any other storage tank. Likewise, simultaneous attacks to both T2 and T5 are expected to result in a severer domino effect than a multi-attack to any other combination of two tanks.

**Table 2**. Out-closeness centrality of the storage tanks shown in Figure 1.

| Storage tank | T1 | T2 | T3 | T4 | T5 | T6 |
|---|---|---|---|---|---|---|
| $C_{out}$ | 0.556 | 0.714 | 0.556 | 0.556 | 0.714 | 0.556 |

For this purpose, we consider a number of single attack (Figures 5(a)-(c)) and double-attack scenarios (Figures 5(d)-(f)), where, for the sake of clarity, the targeted vessels are highlighted.

Modeling the graphs in Figure 5 in igraph [26], the out-closeness scores of the graphs, as an indication of graph vulnerability to domino effects [27], are presented in Table 3 (1st row).

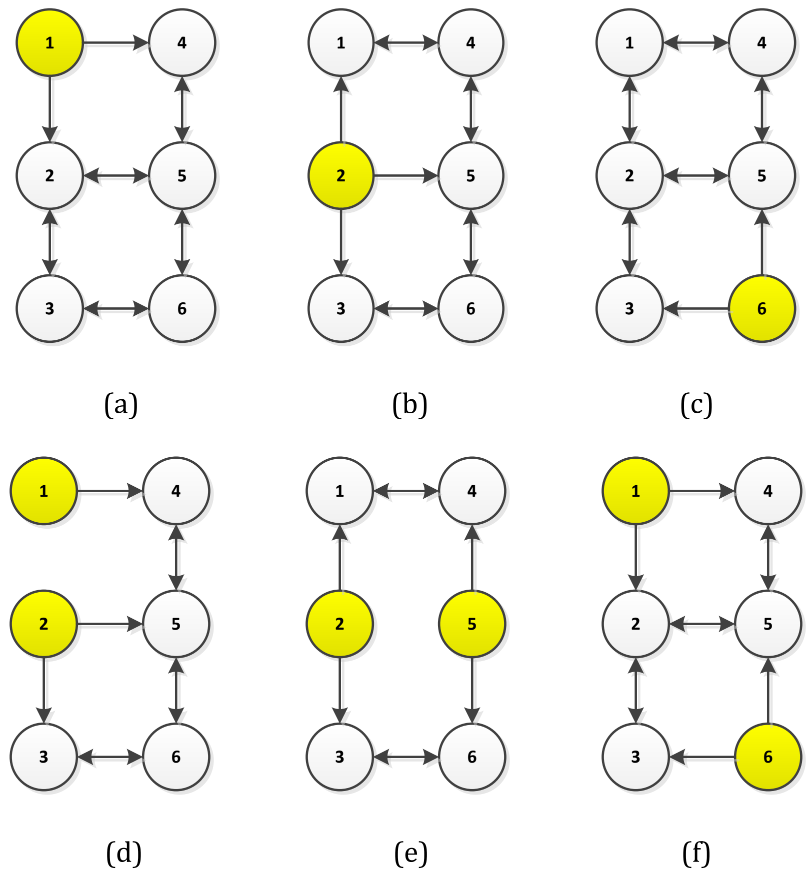


**Figure 5**. (a) Domino effect triggered by attack to T1. (b) Domino effect triggered by attack to T2. (c) Domino effect triggered by attack to T6. (d) Domino effect triggered by attack to T1 and T2. (e) Domino effect triggered by attack to T2 and T5. (f) Domino effect triggered by attack to T1 and T6.

**Table 3**. Graph out-closeness for single-attack and double-attack scenarios depicted in Figure 5.

| | Single-attack | | | Double-attack | | |
|---|---|---|---|---|---|---|
| Graph | Fig. 4(a) | Fig. 4(b) | Fig. 4(c) | Fig. 4(d) | Fig. 4(e) | Fig. 4(f) |
| $C_{out}$ | 0.180 | **0.423** | 0.180 | 0.142 | **0.208** | 0.117 |
| Utility | -42.86 | **-49.45** | -42.86 | -52.81 | **-58.68** | -56.77 |

As can be seen, among single-attack scenarios, the graph presented in Figure 5(b) has the highest graph out-closeness, indicating that a single attack to T2 (or T5) would lead to the severest single-event domino effect[2]. Likewise, among double-attack scenarios, the graph presented in Figure 5(e) has the highest graph out-closeness, indicating that a double-attack to both T2 and T5 would result in the severest double-event domino effect[3]. In the next section, we validate the results obtained from the application of graph metrics using a BN approach.

### 3.2.2. Application of dynamic Bayesian network

We use a methodology based on DBN to model all possible sequences of events during domino effects in the chemical plant [14]. Figure 6 displays the DBN to model possible single- and multiple-event domino effects in the chemical plant of Figure 4(a). The DBN has also been extended to an influence diagram by adding node Utility to the nodes at the last time slice to account for the damage inflicted upon the storage tanks.

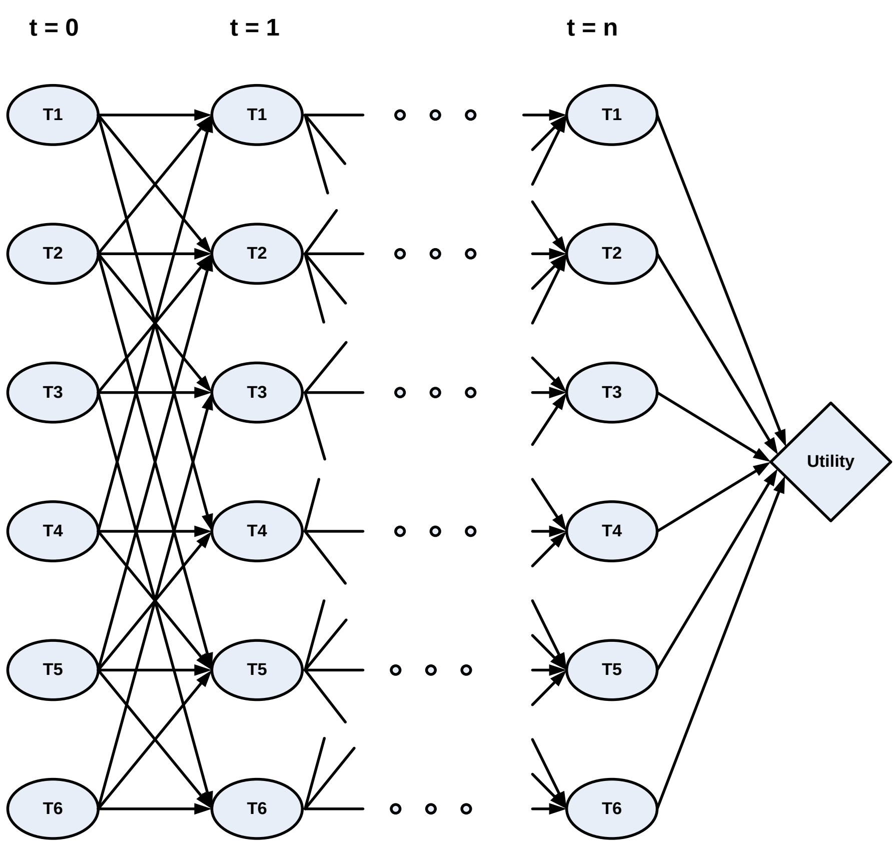


**Figure 6**. Dynamic Bayesian network to model possible sequences of events during domino effects.

---

[2] We use single-event domino effect to refer to domino effects initiating from one primary event (primary vessel).

[3] We use double-event domino effect to refer to domino effects initiating from two primary events (primary vessels).

To model the single-event domino effect triggered by an attack to T1, for example, the state of node T1 at the first time slice, denoted by t = 0, is instantiated to “T1 = Tank fire” while the states of the other nodes at t = 0 are instantiated to “Safe”[4]. Based on the assigned marginal and conditional probabilities, the developed DBN computes unconditional probabilities of the storage tanks at each time slice. For the sake of exemplification, the conditional probabilities assigned to node T4 at 2nd time slice, i.e., t = 1, are reported in Table 4.

In Table 4, the probabilities $P_1$, $P_5$, and $P_{15}$ are also known as escalation probabilities, and can be calculated using a variety of techniques such as probit models [10,11] based on the intensity of escalation vector (e.g., heat radiation) and type and size of target vessels. For the purpose of this study, which is identification of critical vessels based on their relative contribution to domino effects, we use a linear relationship to proportionate the escalation probability to the magnitude of heat radiation. Since a threshold of 15 kW/m$^2$ has been proposed for atmospheric vessels exposed to heat radiation [11], the linear relationship in Equation (8) could be used:

$$P = 1 - \frac{15}{Q} \tag{8}$$

where Q (kW/m$^2$) is the heat radiation received by an atmospheric vessel[5]. As such, for instance, $P_{15}$ = P(T4 $^{t=1}$ = Tank fire | T4 $^{t=0}$ = Safe, T1 $^{t=0}$ = Tank fire, T5 $^{t=0}$ = Tank fire) $= 1 - \frac{15}{Q_{14}+Q_{54}} = 1 - \frac{15}{22+38} = 0.75$ , where $Q_{14}$ and $Q_{54}$ are the heat escalation vectors (kW/m$^2$) T4 receives from T1 and T5, respectively, as listed in Table 1.

[4] In the present study, the storage tanks are considered to have two states, namely “Tank fire” and “Safe”.
[5] A threshold of 45 kW/m$^2$ has been proposed for pressurized vessels exposed to heat [11].

**Table 4**. Conditional probability table of node T4 at t = 1.

| | | | $T4^{t=1}$ | |
|---|---|---|---|---|
| $T4^{t=0}$ | $T1^{t=0}$ | $T5^{t=0}$ | Tank fire | Safe |
| Tank fire | Tank fire | Tank fire | 1 | 0 |
| Tank fire | Tank fire | Safe | 1 | 0 |
| Tank fire | Safe | Tank fire | 1 | 0 |
| Tank fire | Safe | Safe | 1 | 0 |
| Safe | Tank fire | Tank fire | $P_{15}$ | 1 - $P_{15}$ |
| Safe | Tank fire | Safe | $P_1$ | 1 - $P_1$ |
| Safe | Safe | Tank fire | $P_5$ | 1 - $P_5$ |
| Safe | Safe | Safe | 0 | 1 |

In the present study, for illustrative purposes, we assign a (dis)utility of -10.0 to a tank damaged either due to attack with IEDs or due to escalation of subsequent domino effects. Similarly, the utility of a safe tank is 0.0. For example, if an attack to T1 triggers a domino effect involving T2 and T4, the respective utility value incorporated in node Utility in Figure 5 is U (T1 = Tank fire, T2 = Tank fire, T3 = Safe, T4 = Tank fire, T5 = Safe, T6 = Safe) = -30.0.

Running the DBN in GeNIe [28], the expected disutility of single- and double-attack scenarios – due to possible single-event and double-event domino effects that can be triggered by which – are calculated as listed in Table 3 (2nd row). As can be seen, among the single-attack scenarios, the attack to T2 would result in the largest disutility (-49.45) whereas among the double-attack scenarios, the attack to both T2 and T5 would result in the largest disutility (-58.68). Clearly enough, the results of the DBN analysis are in complete agreement with those of graph theoretic approach in the previous section. As a result, in a chemical plant, graph out-closeness can be used as an indication of the plant's vulnerability to domino effects triggered from intentional (or accidental) damage to process vessels.

# Application of the methodology

## 4.1. Vulnerability to intentional domino effects

To demonstrate the application of the methodology, consider the tank farm in Figure 7(a) comprising eight atmospheric storage tanks of oil with diameter of D = 33.5 m, height of H = 15.2 m, and capacity of 9000 $m^3$. Considering tank fires as the primary and secondary events, possible fire escalation patterns during domino effects are presented as the directed graph in Figure 7(b). The intensity of heat radiation between the tanks has been calculated by ALOHA [25] assuming a wind speed of 2 m/s gusting from North, air temperature of 15 $^{o}$C, a partly cloudy sky, and relative humidity of 25%. The out-closeness cores of the tanks are presented in Table 5, with storage tanks 4, 7, and 5 as the ones with the highest out-closeness scores in a descending order.

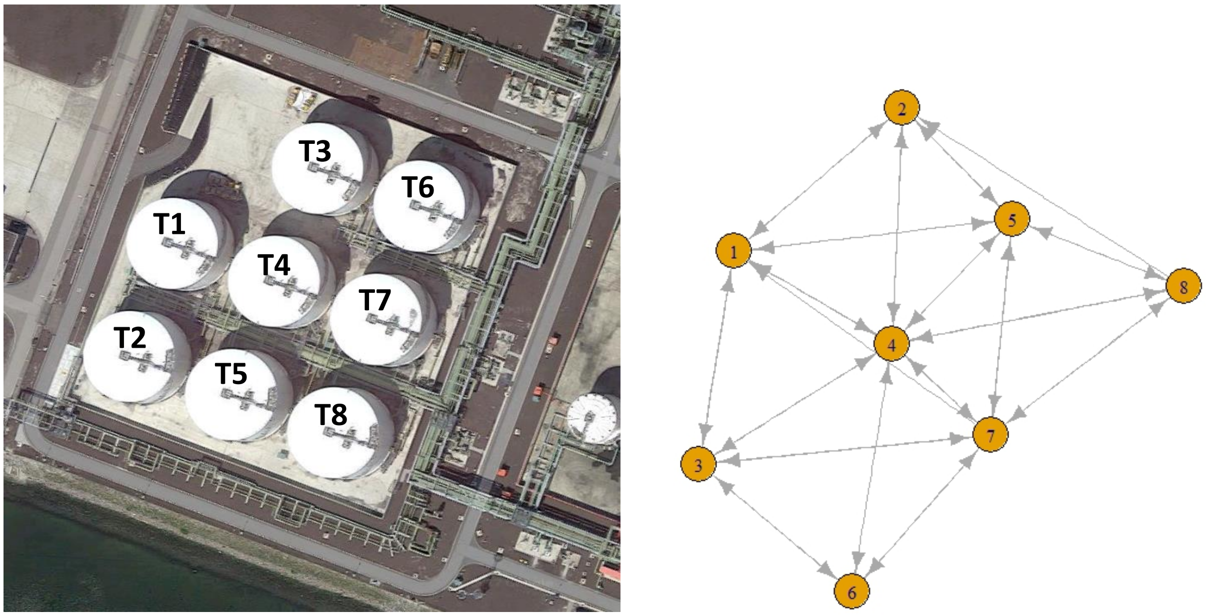


**Figure 7**. (a) Chemical plant consisting of eight atmospheric storage tanks of oil. (b) Possible fire escalation scenarios as a directed graph.

**Table 5**. Out-closeness centrality of the storage tanks shown in Figure 7.

| Storage tank | T1 | T2 | T3 | T4 | T5 | T6 | T7 | T8 |
|---|---|---|---|---|---|---|---|---|
| $C_{out}$ | 0.700 | 0.636 | 0.700 | 1.00 | 0.778 | 0.636 | 0.875 | 0.700 |

## 4.2. Cost-robust design

To prevent or delay the escalation of domino effects, especially in the case of fire propagation, usually a variety of fire protection measures is considered in chemical plants. Fire protection measures can be classified into inherently safer techniques, engineering (passive and active) protection systems, and emergency response measures [29]. Inherently safer techniques such as adequate separation distance among hazardous vessels or adopting less hazardous chemicals and operations [30,31] are among macro-layout changes which are usually applicable to design stage of chemical plants. Where macro-layout changes are not possible, micro-layout modifications such as adding passive and active protection systems can be considered, including sprinkler systems, water deluge systems, emergency shut down systems, and fireproofing [32]. Emergency response measures such as firefighting can be integrated with engineering protection systems to further delay and control of fire escalation.

In the present study, low-capacity utilization of chemical plants as a way of increasing their robustness against intentional domino effects is examined. Provisionally reducing the inventory of hazardous chemicals in face of imminent terrorist attacks can significantly reduce the severity and extent of damage. Since low-capacity utilization of a chemical plant can inflict losses in the form of, among others, loss of revenue or adverse impacts on downstream industries and supply chain, it should be performed based on a cost-benefit analysis. Since the benefit gained from such low-capacity utilization would be an increase in the robustness of the plant, we refer to it as a cost-robust analysis instead.

Based on the out-closeness scores of the storage tanks in Table 5 as an indication of their criticality in intentional attacks, a number of plans can be considered for low-capacity utilization of the plant. The plans, their costs and resulting plant out-closeness scores as an implication of plant robustness have been listed in Table 6. To calculate the graph out-closeness resulted from implementation of each plan, the escalation vectors emitting from respective storage tank(s) have been removed from the graph in Figure 7(b) and the modified graph's out-closeness has been recalculated. For example, since T4 would be empty for Plan 1, there would not be any directed arcs (escalation vectors) from T4 to the other storage tanks (nodes) in the graph even if T4 is damaged under attack. As can be seen from Table 6, the plant's out-closeness decreases with an increase in the number of empty tanks.

**Table 6**. Low-capacity utilization plans.

| Plan ID | Description | Graph $C_{out}$ | Cost (€) |
|---|---|---|---|
| 0 | No tank is empty | 0.322 | 0 |
| 1 | T4 is empty | 0.291 | 1000 |
| 2 | T4 & T7 are empty | 0.282 | 2718 |
| 3 | T4, T7 & T5 are empty | 0.169 | 7389 |
| 4 | T4, T5, T7 & T1 are empty | 0.091 | 20085 |

In order to calculate the cost of each plan, we, for illustrative purposes, assume that the cost the plant incurs due to operating under lower capacity can be estimated using an exponential relationship as presented in Equation (9).

$$C = 1000\ \exp(n - 1) \tag{9}$$

where C is the cost (Euro), and n is the number of empty tanks. Equation (9) implies the cost aversion [33] of the plant which grows exponentially with lowering the capacity of the plant. Having the cost and graph out-closeness of the plans, "reference-point" optimization technique (Figure 8) can be used to identify the optimal cost-robust plan for low-capacity utilization of the plant in face of imminent terrorist attacks. As displayed in Figure 8, the point with the lowest cost and highest robustness (the lowest graph out-closeness) is presented as Utopia the closest node to which can be identified as the optimal plan. Using Equation (7), Plan 1 (to empty tank T4) turns out to have the shortest distance to Utopia, and thus being identified as the optimal cost-robust strategy.

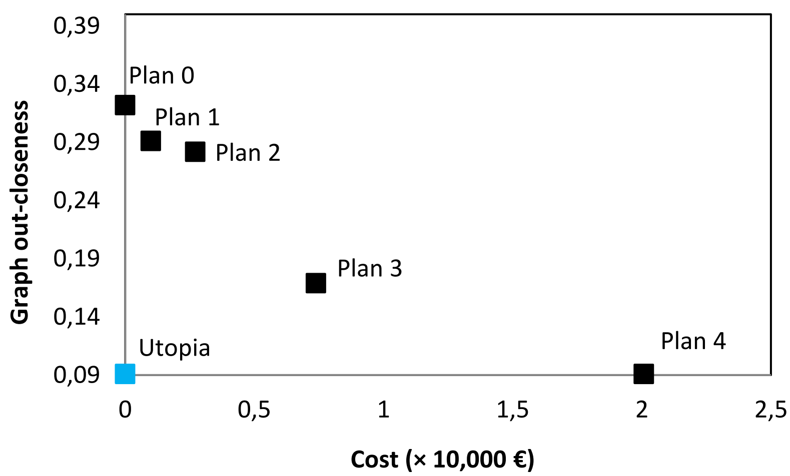


Figure 8. Application of reference-point decision making to identify optimal strategy for low-capacity utilization.

## Conclusions

In the present study we employed graph theory to assess the vulnerability of chemical plants to domino effects triggered by intentional attacks. We also used a methodology based on dynamic Bayesian network to validate the graph theoretic approach. Applying both graph theoretic and dynamic Bayesian approaches, it was demonstrated that simultaneous attack to process vessels with highest out-closeness score would result in more extensive domino effects, thus causing maximum damage within the plant. In this regard, a plant's average out-closeness score was illustrated to represent the plant's vulnerability (robustness) to intentional domino effects. Furthermore, we proposed low-capacity utilization of chemical plants as a way of reducing their vulnerability to intentional domino effects in the case of impending intentional attacks (for example, in the case of elevated or imminent alerts [34]). To determine the optimal low-capacity utilization plan, we employed the reference-point optimization technique to make a trade-off between the cost the plant incurs and the robustness the plant gains due to low-capacity utilization. Although the focus of the present study has been on intentional domino effects, the developed methodology – both graph theoretic and dynamic Bayesian network approaches – can be applied to accidental domino effects without any alteration.

## References

[1] RAND Database of Worldwide Terrorism Incidents. Available online at: https://www.rand.org/nsrd/projects/terrorism-incidents.html. Last checked on July 11, 2017.

[2] Khan FI, Abbasi SA. Models for domino effect analysis in chemical process industries. Process Safety Progress, 1998; 17: 107–23.

[3] Arturson G. The tragedy of San Juanico - the most severe LPG disaster in history. Burns Including Thermal Injury, 1987; 13(2): 87–102.

[4] BBC. 2010. How the Buncefield fire happened. http://www.bbc.com/news/uk-10266706. Last checked on July 11, 2017.

[5] U.S. Chemical Safety Board (CSB). 2015. Caribbean Petroleum Refining Tank Explosion and Fire. http://www.csb.gov/caribbean-petroleum-refining-tank-explosion-and-fire. Last checked on July 11, 2017.

[6] BBC News. 15 July 2015. France explosions: Devices found near Berre-L'Etang plant. Available from www.bbc.com/news/world-europe-33537345. Last checked on May 16, 2017.

[7] Delvosalle C. A methodology for the identification and evaluation of domino effects. Brussels, Belgium: Belgian Ministry of Employment and Labour; 1998.

[8] Gledhill J, Lines I. Development of methods to assess the significance of domino effects from major hazard sites. London, UK: Health and Safety Executive, HM Stationery Office; 1998.

[9] Bagster DF, Pitblado RM. Estimation of domino incident frequencies - an approach. Process Safety and Environmental Protection, 1991; 69: 195–199.

[10] Cozzani V, Gubinelli G, Antonioni G, Spadoni G, Zanelli S. The assessment of risk caused by domino effect in quantitative area risk analysis. Journal of Hazardous Materials, 2005, A127, 14–30.

[11] Landucci G, Gubinelli G, Antonioni G, Cozzani V. The assessment of the damage probability of storage tanks in domino events triggered by fire. Accident Analysis and Prevention, 2009; 41: 1206–1215.

[12] Nguyen QB, Mebarki A, Saada RA, Mercier F, Reimeringer M. Integrated probabilistic framework for domino effect and risk analysis. Advance Engineering Software, 2009; 40: 892–901.

[13] Khakzad N, Khan F, Amyotte P, Cozzani V. Domino effect analysis using Bayesian networks. Risk Analysis, 2013; 33: 292–306.

[14] Khakzad N. Application of dynamic Bayesian network to risk analysis of domino effects in chemical infrastructures. Reliability Engineering and System Safety, 2015; 138: 263–272.

[15] Reniers G, Dullaert W, Audenaert A, Ale B, Soudan K. Managing domino effect-related security of industrial areas. Journal of Loss Prevention in the Process Industries, 2008; 21: 336–343.

[16] Reniers G, Audenaert A. Preparing for major terrorist attacks against chemical clusters: Intelligently planning protection measures w.r.t. domino effects. Process Safety and Environmental Protection, 2014; 92: 583–589.

[17] Landucci G, Reniers G, Cozzani V, Salzano E. Vulnerability of industrial facilities to attacks with improvised explosive devices aimed at triggering domino scenarios. Reliability Engineering and System Safety, 2015, 143, 53-62.

[18] Von Neumann J, Morgenstern O. Theory of Games and Economic Behavior, Princeton University Press, Princeton, New Jersey, 1953.

[19] Pate-Cornell E, Guikema S. Probabilistic modeling of terrorist threats: A system analysis approach to setting priorities among countermeasures. Military Operations Research, 2002, 7(4), 5-20.

[20] Khakzad N, Reniers G. Using graph theory to analyze the vulnerability of process plants in the context of cascading effects. Reliability Engineering and System Safety, 2015, 143, 63–73.

[21] Freeman LC. Centrality in social networks I: conceptual clarification. Social Networks, 1979, 1, 215–239.

[22] Pearl J. Probabilistic reasoning in intelligent systems. San Francisco, CA: Morgan Kaufmann; 1988.

[23] Neapolitan R. 2003. Learning Bayesian Networks. Prentice Hall, Inc., Upper Saddle River, NJ, USA.

[24] Deb K. 2001. Multi-Objective Optimization using Evolutionary Algorithms. New York, NY: John Wiley & Sons.

[25] ALOHA. US Environmental Protection Agency, National oceanic and atmospheric administration, ALOHA, Version 5.4.4., November 2015, available on line at: http://www.epa.gov/OEM/cameo/aloha.htm. Last checked July 12, 2017.

[26] Csardi G, Nepusz T. The igraph software package for complex network re search. International Journal of Complex Systems, 2006, 1695.

[27] Khakzad N, Reniers G, Abbassi R, Khan F. Vulnerability analysis of process plants subject to domino effects. Reliability Engineering and System Safety, 2016, 154, 127–136.

[28] GeNIe. Decision Systems Laboratory, University of Pittsburg, available online at: https://www.bayesfusion.com. Last checked July 12, 2017.

[29] CCPS - Center of Chemical Process Safety. 2001. Layer of protection analysis: simplified process risk assessment. New York, NY: American Institute of Chemical Engineers.

[30] Hendershot DC. Inherently safer chemical process design. Journal of Loss Prevention in Process Industries, 1997;10:151–7.

[31] Kletz TA, and Amyotte P. 2010. Process Plants: A Handbook for Inherently Safer Design, 2nd ed., CRC Press, Boca Raton, FL. ISBN 9781439804551.

[32] Landucci G, Argenti F, Tugnoli A, Cozzani V. Quantitative assessment of safety barrier performance in the prevention of domino scenarios triggered by fire. Reliability Engineering & System Safety 2015; 143: 30-43.

[33] Gilboa I. 2009. Theory of Decision under Uncertainty. Cambridge University Press, New York, USA, ISBN 978-0-521-51732-4.

[34] U.S. Department of Homeland Security. National Terrorism Advisory System Bulletin. Available online at: https://www.dhs.gov/ntas/advisory/ntas_17_0515_0001. Last checked July 12, 2017.